Molecular Cell
Article

SR Protein Family Members Display Diverse Activities in the Formation of Nascent and Mature mRNPs In Vivo

Aparna K. Sapra,[1] Minna-Liisa Änkö,[1] Inna Grishina,[1] Mike Lorenz,[1] Marta Pabis,[1] Ina Poser,[1] Jarod Rollins,[1] Eva-Maria Weiland,[1] and Karla M. Neugebauer[1,*]
[1]Max Planck Institute of Molecular Cell Biology and Genetics, Pfotenhauerstrasse 108, 01307 Dresden, Germany
*Correspondence: neugebau@mpi-cbg.de
DOI 10.1016/j.molcel.2009.02.031

SUMMARY

The SR proteins are a family of pre-mRNA splicing factors with additional roles in gene regulation. To investigate individual family members in vivo, we generated a comprehensive panel of stable cell lines expressing GFP-tagged SR proteins under endogenous promoter control. Recruitment of SR proteins to nascent *FOS* RNA was transcription dependent and RNase sensitive, with unique patterns of accumulation along the gene specified by the RNA recognition motifs (RRMs). In addition, all SR protein interactions with Pol II were RNA dependent, indicating that SR proteins are not preassembled with Pol II. SR protein interactions with RNA were confirmed in situ by FRET/FLIM. Interestingly, SC35-GFP also exhibited FRET with DNA and failed to associate with cytoplasmic mRNAs, whereas all other SR proteins underwent nucleocytoplasmic shuttling and associated with specific nuclear and cytoplasmic mRNAs. Because different constellations of SR proteins bound nascent, nuclear, and cytoplasmic mRNAs, mRNP remodeling must occur throughout an mRNA's lifetime.

INTRODUCTION

The SR protein family consists of seven canonical members—ASF/SF2, SC35, 9G8, SRp20, SRp40, SRp55, and SRp75—originally identified for their activities as constitutive and alternative pre-mRNA splicing factors (Lin and Fu, 2007). The SR proteins are highly conserved and are characterized by one or two RNA recognition motifs (RRMs) at their N termini and a highly phosphorylated region of serine-arginine repeats, the RS domain, at their C termini. While the RRMs can bind RNA sequence specifically, the RS domain may mediate protein-protein interactions and/or contact RNA (Blencowe, 2006; Shen and Green, 2006; Shen et al., 2004; Wu and Maniatis, 1993). The RS domain is also a target of a network of kinases, which can modulate the activities of SR proteins in response to signaling (Blaustein et al., 2005; Sanford et al., 2005). These structural and functional properties are not only important for splicing but play additional roles in RNA processing. SF2 has been implicated in mRNA translation, while SRp20 and 9G8 are required for nuclear export mRNA (Hautbergue et al., 2008; Huang et al., 2003; Huang and Steitz, 2001; Sanford et al., 2004). SF2 and/or SC35 have now also been implicated in oncogenesis, genome instability, and transcriptional elongation (Karni et al., 2007; Li and Manley, 2005; Li et al., 2005; Lin et al., 2008; Xiao et al., 2007).

While splicing itself is carried out by the spliceosome, the identification of intron-exon boundaries in metazoans requires the activity of *trans*-acting factors (Wahl et al., 2009). The SR proteins were identified as proteins that could complement a splicing-deficient S100 extract, using constitutively spliced pre-mRNAs (Fu and Maniatis, 1990; Ge and Manley, 1990; Krainer et al., 1990; Zahler et al., 1992). Over the years, it has emerged that SR proteins promote exon definition by enhancing recruitment of the U1 snRNP to 5′ splice sites and the U2 snRNP to 3′ splice sites; thereby, SR protein binding can lead to the recognition of exons that have poor 5′ and 3′ splice site sequences compared to consensus (Blencowe, 2006; Lin and Fu, 2007; Matlin et al., 2005). Current models hold that SR proteins regulate alternative splicing by binding to specific RNA sequence elements, called exonic splicing enhancers (ESEs), 5–10 nucleotide long degenerate sequences that are distributed at a high frequency in the genome (Blencowe, 2006; Hertel, 2008). However, because SR proteins are expressed at high concentrations in most cells, the sequence specificity of SR protein binding in vivo is currently unclear.

In cells, SR proteins are primarily nucleoplasmic and concentrated in nuclear speckles, leading to an early proposal that nuclear speckles are the sites of splicing (Fu and Maniatis, 1990; Lamond and Spector, 2003). This was at odds with data showing that splicing occurs while the gene is still being transcribed, i.e., cotranscriptionally (Neugebauer, 2002). Live cell imaging experiments resolved this controversy, showing that SR proteins are recruited to genes throughout the nuclear volume from a mobile pool (Lewis and Tollervey, 2000; Mabon and Misteli, 2005; Misteli et al., 1997; Neugebauer and Roth, 1997). The transcription unit, therefore, is the nucleation point for transacting factors that initiate RNA processing steps during transcription (Kornblihtt, 2006; Neugebauer, 2002). Coupled transcription and splicing assays have been developed in vitro and support direct links between RNA polymerase II (Pol II) transcription and splicing, though it is still controversial whether this effect is due to an enhancement of splicing or of (pre-) mRNA stability (Das et al., 2006; Ghosh and Garcia-Blanco, 2000; Hicks

et al., 2006; Lazarev and Manley, 2007). This has led to the hypothesis that careful orchestration of the machineries involved affords the cell a temporal and spatial advantage in regulating the transcripts emerging from transcription units (Moore and Proudfoot, 2009).

An unresolved question is whether SR proteins are recruited to sites of transcription by their affinity for nascent RNA alone or whether SR proteins are already preassembled with Pol II and/or the spliceosomal snRNPs. The possibility that SR proteins bind directly to Pol II first arose with the insight that the Pol II C-terminal domain (CTD) would provide an ideal platform for the binding of these highly charged splicing factors. Indeed, the efficiency of splicing and alternative splice site selection depends on the speed of the elongating Pol II; in addition, the Pol II CTD is required for the action of certain SR proteins (Batsche et al., 2006; de la Mata et al., 2003; de la Mata and Kornblihtt, 2006; Kornblihtt, 2006; Listerman et al., 2006; Misteli and Spector, 1999). Evidence that Pol II and SR proteins can coimmunoprecipitate seems to argue for a stable complex between SR proteins and Pol II (Du and Warren, 1997; Robert et al., 2002). This evidence contrasts with mass spectrometry studies, which find that Pol II and SR proteins are *not* correlated in biochemical purifications of either Pol II holoenzyme or spliceosomes (Jeronimo et al., 2007; Jurica et al., 2002; Makarov et al., 2002; Rappsilber et al., 2002; Zhou et al., 2002). Moreover, recent evidence has raised the possibility that the association may be indirect, linked via the U1 snRNP, rather than directly through the CTD (Das et al., 2007; Natalizio et al., 2009; Wu and Maniatis, 1993). One explanation for these divergent observations is that the conditions vary among in vitro assays. Therefore, in vivo approaches are necessary to determine how SR proteins accumulate at active genes.

Cotranscriptional assembly of SR proteins on nascent RNAs has not been directly observed with high-resolution methods. Therefore, we set out to examine SR protein accumulation on chromatin by "splicing factor ChIP," in which the distribution of splicing factors along genes is assayed by in vivo crosslinking and ChIP. This method has made cotranscriptional spliceosome assembly and splicing accessible in *Saccharomyces cerevisiae* and mammalian tissue culture cells (Gornemann et al., 2005; Lacadie and Rosbash, 2005; Listerman et al., 2006). Due to a lack of specific antibodies against all members of the SR protein family, we sought a strategy for tagging with a universal epitope. SR proteins have previously been tagged and expressed as cDNAs driven by strong promoters, and this can alter splicing outcome due to overexpression (Caceres et al., 1994; Wang and Manley, 1995). Therefore, we used bacterial artificial chromosomes (BACs) to express GFP-tagged versions of six members of the SR protein family: SRp20 (gene name SFRS3), ASF/SF2 (SFRS1, hereafter referred to as SF2 for simplicity), SC35 (SFRS2), 9G8 (SFRS7), SRp55 (SFRS6), and SRp75 (SFRS4). BACs carrying the SR protein genes of choice were site-specifically recombineered to introduce the GFP tag prior to the stop codons and used to generate stable HeLa cell lines (Poser et al., 2008). Each SR protein-encoding gene, including introns, is expressed under the control of its own promoter similar to the endogenous gene, and the GFP tag facilitates biochemical and cell biological analysis with the same α-GFP antibody. The present study provides a comprehensive analysis of SR protein behavior and reveals inherent differences among family members.

RESULTS

We previously established splicing factor ChIP in mammalian cells, using antibodies specific for endogenous splicing factors to localize the U1 snRNP, U2AF65, and the U5 snRNP to the human *FOS* gene (Listerman et al., 2006). We used BAC recombineering to add C-terminal GFP tags to these and other splicing factors of interest; this maintains endogenous expression levels and permits the use of a single antibody for each ChIP. Figure 1A shows the profile of GFP-tagged U1-70K (U1 snRNP), U2AF65, and hPrp8 (U5 snRNP) on the induced *FOS* gene in stable, individually tagged HeLa cell lines. In comparison with the prior study (Listerman et al., 2006), the pattern of each component along *FOS* is nearly identical to the pattern observed with direct antibodies. When possible, we compared the level of each splicing factor with endogenous levels (Figure 1B); GFP-tagged protein levels among stably transformed cell clones were equivalent to or lower than the endogenous protein.

The GFP tag enabled us to verify and extend analysis of the cellular behavior of SR proteins in situ. First, we verified the nuclear localization pattern of the tagged splicing factors (Figure 1C). Second, nucleocytoplasmic shuttling was tested, because U2AF65, SF2, SRp20, and 9G8 are known to shuttle between the nucleus and cytoplasm, while SC35 is retained in the nucleus (Caceres et al., 1998; Gama-Carvalho et al., 2001). The other SR proteins have not yet been assayed. Inspection of the images reveals that U2AF, SRp20, and 9G8 shuttle most robustly, consistent with their previously demonstrated roles in nuclear export of mRNA (Figure 1C). Interestingly, SRp55 and SRp75 also shuttled, but the intensities of the receiving nuclei were relatively dimmer. This level of shuttling was significant, because the intensities of the receiving nuclei were consistently higher than those observed with Prp8 and SC35, which did not shuttle in this assay. Third, we tested whether the GFP-tagged SR proteins localize to rounded-up speckles when transcription is inhibited (Lamond and Spector, 2003); all redistributed as expected upon α-amanitin treatment (see Figure S1 available online). Fourth, we tested recruitment to a known target; 9G8—but not SRp20, SC35, SRp55, or SRp75—was recruited to SAT III loci upon activation by stress (Figure S2), consistent with prior results (Denegri et al., 2001). We conclude by these criteria—correct patterns of accumulation on *FOS*, expression levels, and correct subcellular localization and dynamics—that use of BACs to introduce GFP-tagged splicing factors leads to physiological behavior.

We next tested whether the GFP tag could be used to localize SR proteins on chromatin. Note that immunoprecipitation of each tagged SR protein with α-GFP did not pull down other SR protein family members (data not shown); thus, results obtained with GFP as an affinity tag are specific for the indicated protein. To determine whether SR proteins are recruited to *FOS*, ChIP was performed in the panel of stable cell lines. SRp20, SF2, SC35, 9G8, SRp55, and SRp75 accumulated on the *FOS* gene exclusively upon induction (Figure 2). ChIP signals obtained with α-GFP for tagged 9G8 and SF2 were more robust

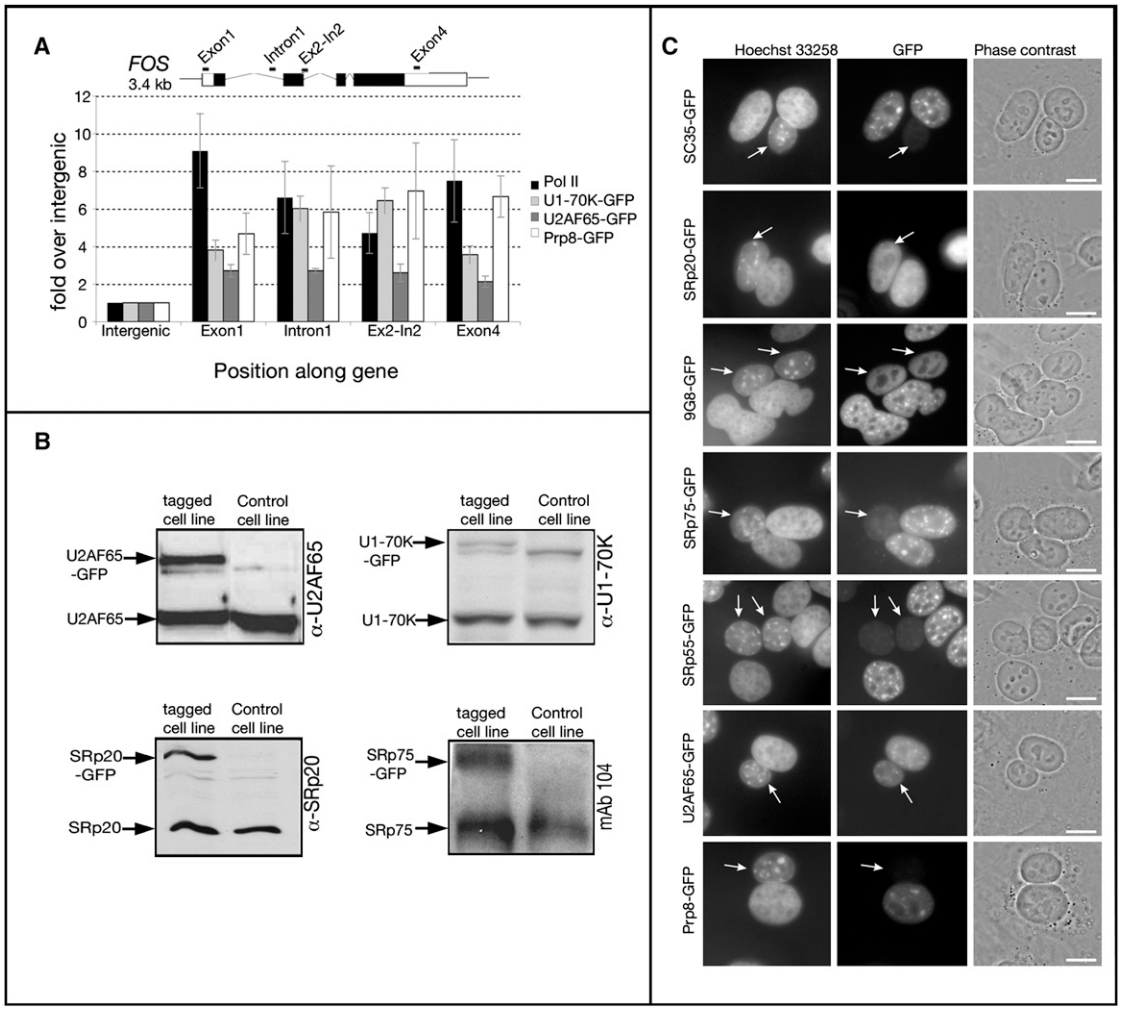

Figure 1. Stable Expression of GFP-Tagged Splicing Factors from Recombineered BACs in HeLa Cells

(A) Proof-of-principle ChIP experiment, using α-GFP antibodies to detect GFP-tagged U1-70K, U2AF65, and Prp8 proteins, each expressed from BACs in stable cell lines. The profiles show that the use of the tag permits robust detection of each splicing factor in the expected pattern along activated *FOS*. Cartoon representing *FOS* gene structure is shown.

(B) Physiological expression levels of tagged proteins were verified by western blot analysis of different single-cell stable clones and untransfected control cells (HeLa), comparing expression levels of GFP-tagged and endogenous proteins. Antibodies to SRp20 (7B4), all SR proteins (104), and U2AF65 (MC3) were used.

(C) The nucleocytoplasmic shuttling of different splicing factors and SR proteins was assayed in heterokaryons after fusion of splicing factor GFP-stable HeLa cells to mouse NIH 3T3 cells (marked by an arrow) and 4 hr translation inhibition. Nuclei were stained with Hoechst 33258. The appearance of GFP signal in mouse nuclei shows that the indicated protein was exported from the HeLa cell nucleus and reimported from the common cytoplasm into the mouse cell nucleus. Scale bar, 10 μm.

than those obtained with antibodies that bind endogenous 9G8 and SF2, but the patterns were similar (Figure S3). Thus, the tag does not disrupt function and sometimes enhances detection, perhaps due to better accessibility. Despite this sensitivity, none of the SR proteins was detected at the promoter of uninduced *FOS*, where Pol II was highly concentrated, indicating that SR proteins are not preloaded on *FOS* with paused Pol II.

Interestingly, the pattern of accumulation along *FOS* differed among the SR proteins. SRp20 signal is highest in exon 1 and decreases from ~7-fold to only ~3-fold above background in exon 4, suggesting either that SRp20-binding sites are spliced out or that the mRNP is remodeled during transcription. In contrast, SRp55 is detected 4-fold above background in exon 1 but increases to 10-fold by exon 4; this suggests that SRp55 binding increases toward downstream gene regions. A sequence-based search revealed many potential ESEs along *FOS* (Wang et al., 2005); however, the densities of the scores did not correlate well with ChIP patterns (Figure S4). Similarly, SC35 was highly detectable on the induced heat shock gene *HSPA1B*, yet predicted SC35 ESEs were no more abundant than those for SRp55, which was not recruited to this intronless gene (Figure S4). Thus, we do not observe a correlation between cotranscriptional SR protein accumulation and predicted target sites. Note that the compact architecture of the *FOS* gene precludes the precise assignment of potential binding sites based on ChIP data; binding of SR proteins to 5′ regions of the

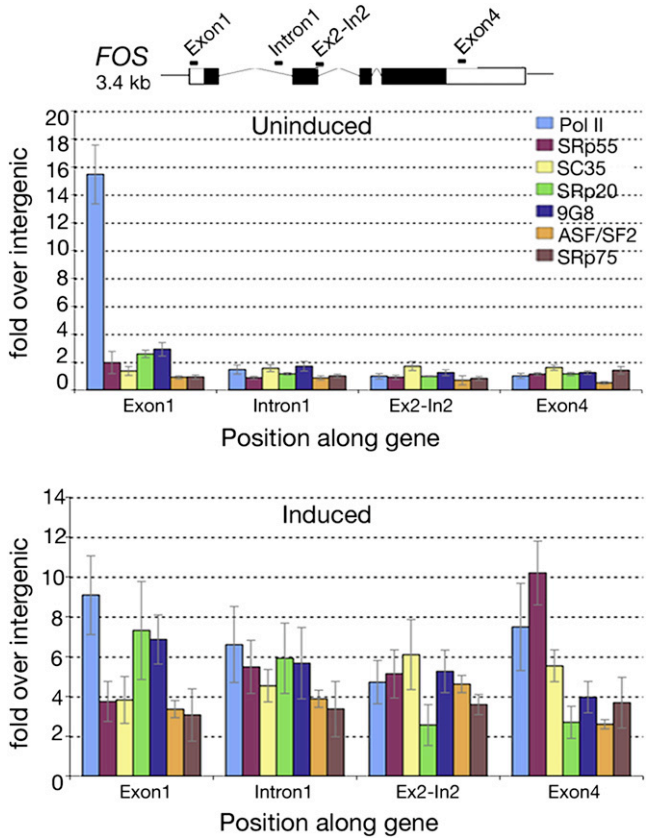

Figure 2. Cotranscriptional Recruitment of SR Proteins to the *FOS* Gene Is Transcription Dependent In Vivo

ChIP profiles of Pol II and GFP-tagged members of the SR protein family (shown in key) on *FOS* uninduced (top panel) and transcriptionally induced (bottom panel). Cartoon representing *FOS* gene structure is shown above the panels. Amplicons distributed within each gene are marked by horizontal black bars, which are centered over the following positions in the gene: +179, +945, +1373, and +2850. The y axis in each graph denotes fold over intergenic, the signal obtained from a region marked as gene desert (Listerman et al., 2006). The x axis shows the amplicons corresponding to the cartoon above. Each data point represents the mean of four to seven biological replicates, and errors are SEM.

pre-mRNA may persist along the gene, since the entire pre-mRNA is transported to the termination site by Pol II. We conclude that individual SR proteins assemble in unique patterns on *FOS*, and active transcription is required.

To understand how the pattern of SR proteins on active *FOS* is established, we determined the relative contribution of the RRM compared to the RS domain. We examined SRp55 and SRp20, because they exhibited distinctive accumulation patterns on *FOS* when the tagged proteins were expressed from BACs (Figure 3A). First, GFP fusions between SRp55RRM and SRp55RS domains were cloned for transient expression (Figure 3B). Although both fusion proteins were well expressed (data not shown), neither was detected on active *FOS* by ChIP (Figure 3B). Because transiently transfected, full-length SRp55-GFP did accumulate on active *FOS* in a pattern similar to that revealed with the BAC construct, we conclude that both protein domains are required for cotranscriptional binding. Next, domain-swapping experiments were carried out. Interestingly, when SRp55-RS was fused with SRp20-RRM, the recruitment profile mimicked that of SRp20 rather than that of SRp55. In contrast, SRp20RS fused with SRp55RRM behaved like SRp20 (data not shown). We conclude that, although the RS domain is required for cotranscriptional recruitment of the protein to *FOS*, the RRM specifies the pattern of recruitment.

Because SR protein accumulation on the *FOS* gene depends on transcriptional activity and the RRM, a direct interaction between the SR proteins and the nascent RNA is implied. Alternatively, it is possible that the SR proteins associate with elongating Pol II in an RRM-dependent manner. To test this directly, we determined the effect of RNase treatment on the association of SRp55-GFP with active *FOS*. In parallel, ChIPs for Pol II and the cap-binding complex (CBC) were performed as negative and positive controls, respectively. We expected detection of the CBC, which binds directly to the 7-methyl-guanosine cap on the 5′ end of nascent RNA, to be fully RNase sensitive. Figure 4 shows that RNase A treatment reduced the signal for CBP80 and SRp55 by up to 80%. In contrast, Pol II showed only a mild decrease in signal upon RNase treatment. This indicated that the majority of the signal detected for SRp55 was mediated through its association with the emerging RNA or another RNase-sensitive protein complex. The residual signal could be due to protein-protein interactions and/or an inability to completely digest the crosslinked RNA.

As a more general approach to the question of how SR proteins interact with chromatin, we employed an assay that detects protein-RNA or protein-DNA proximity in situ by fluorescence resonance energy transfer (FRET). The GFP tag of the SR protein serves as the fluorescence donor and the RNA- and DNA-intercalating dye SytoxOrange as the acceptor (Lorenz, 2009). FRET, measured here by fluorescence lifetime imaging microscopy (FLIM), only occurs if the fluorophores are 2–10 nm apart and in a favorable orientation with respect to one another; a negative result (e.g., SF2-GFP) cannot be interpreted as a failure to interact. The fluorescence lifetime of the donor (GFP) measured in absence of the acceptor (SytoxOrange; Figures 5A and 5E) decreases upon dye addition if FRET occurs, indicating an association of the GFP-tagged SR protein with either RNA or DNA (Figures 5B and 5F). FRET was detected between SytoxOrange and SRp20, SRp75, and SC35. For SRp20 and SRp75, FRET was abolished by RNase A digestion but was unchanged after treatment with DNase I, indicative of interactions with RNA and not DNA. In contrast, SC35-GFP FRET with SytoxOrange was sensitive to both RNase A and DNase I, suggesting that SC35 associates more closely with DNA than the other SR proteins. As a specificity control, RNase A and DNase I had no effect on the fluorescence lifetime of SF2-GFP, which did not FRET with SytoxOrange. Overall, this independent assay validates our conclusion that SR proteins interact closely with RNA.

Taken together, our data from the ChIP and FRET experiments suggest that SR proteins accumulate on active genes via direct RNA binding rather than by binding to Pol II. To determine whether SR proteins stably interact with Pol II by another means, we performed α-GFP pull-down experiments without prior crosslinking. We anticipated that RNA-dependent as well as

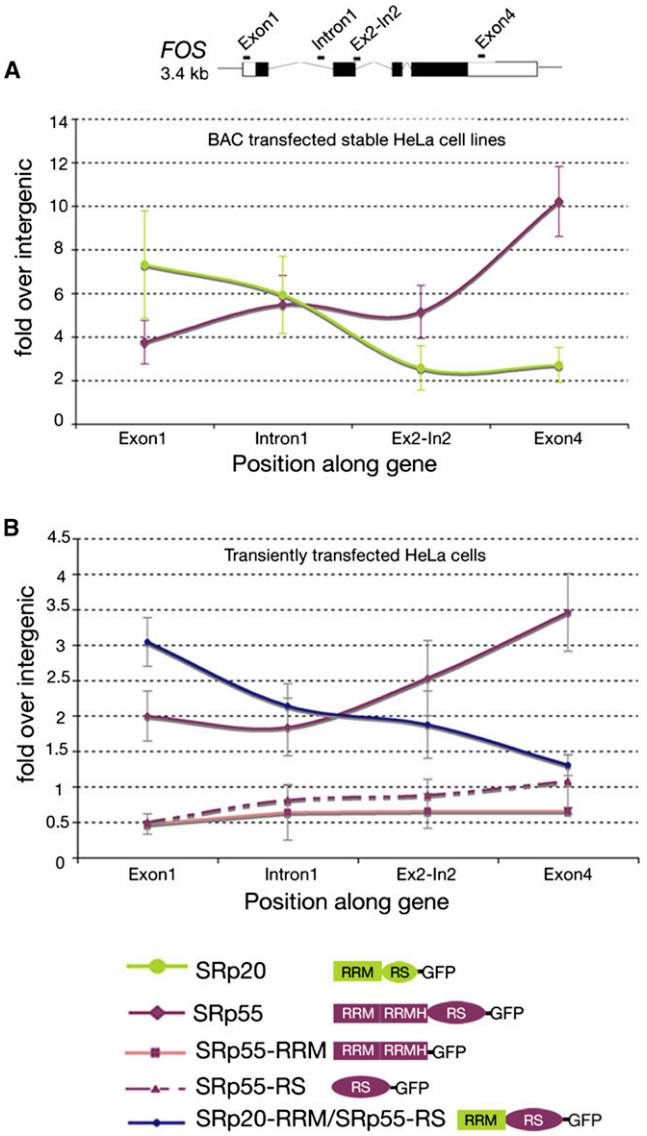

Figure 3. Cotranscriptional Accumulation of SR Proteins Is Specified by the RRM Domain

(A) ChIP profiles of SRp20-GFP (green) and SRp55-GFP (red) expressed from BACs; data are replotted from Figure 2 as a line diagram to emphasize the pattern of accumulation of each protein along activated *FOS*.

(B) ChIP profiles of SRp55-GFP (red), SRp55RRM-GFP (light red), SRp55RS-GFP (dashed red), and SRp20RRM-SRp55RS-GFP (blue) constructs on induced FOS, following transient transfection. Diagrams of the fusion proteins expressed transiently for ChIP experiments are shown below. Each data point represents the mean of three to four biological replicates; errors are SEM.

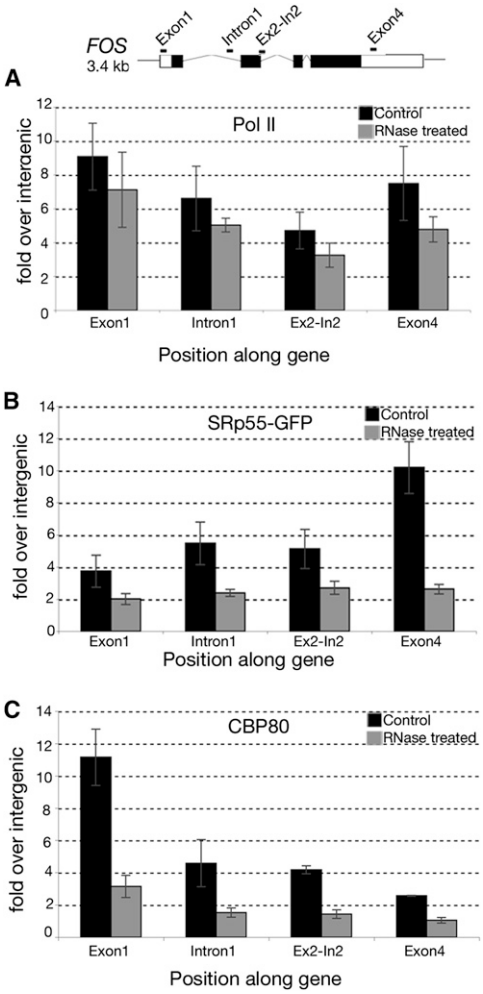

Figure 4. SRp55 Accumulation on the Active *FOS* Gene Is RNA Dependent

ChIP results for (A) Pol II (mAb Pol 3/3), (B) SRp55-GFP (α-GFP), and (C) CBP80 on induced *FOS*, following treatment of the crosslinked extracts with (gray) or without (black) RNase A. Each data point represents the mean of four to seven biological replicates; errors are SEM.

RNA-independent interactions might be observed; the RNA-dependent interactions would be RNase sensitive and represent either cotranscriptional or posttranscriptional RNP complexes, while direct protein-protein interactions would be RNase insensitive (Figure 6A). All SR proteins associated with the CBC and coimmunoprecipitate both the CBP80 and CBP20 subunits (Figure 6B). Association with Pol II, detected by western blot with antibody-specific multiple phosphorylation states of the CTD, was evident for SRp55, SC35, ASF/SF2, and SRp75 but not SRp20 or 9G8 (Figure 6B and Figure S5). Interestingly, all of the above associations were abolished by RNase treatment. In contrast, CBP20 association with CBP80 was not sensitive to RNase, showing that RNase treatment did not disrupt direct protein-protein interactions. These results indicate that, even under conditions that preserve SR protein interactions with (pre-)mRNA, SR proteins do not stably bind to either CBC or Pol II.

It has been proposed that SR proteins are recruited to transcription units by binding to the U1 snRNP, which is in turn bound to Pol II (Das et al., 2007). Because the snRNP integrity depends on the snRNA, we could not assay RNase sensitivity. Nevertheless, we screened for SR protein interactions with snRNPs carefully in two ways, using the same conditions as those in Figure 6B. First, α-GFP pull-downs were probed for endogenous

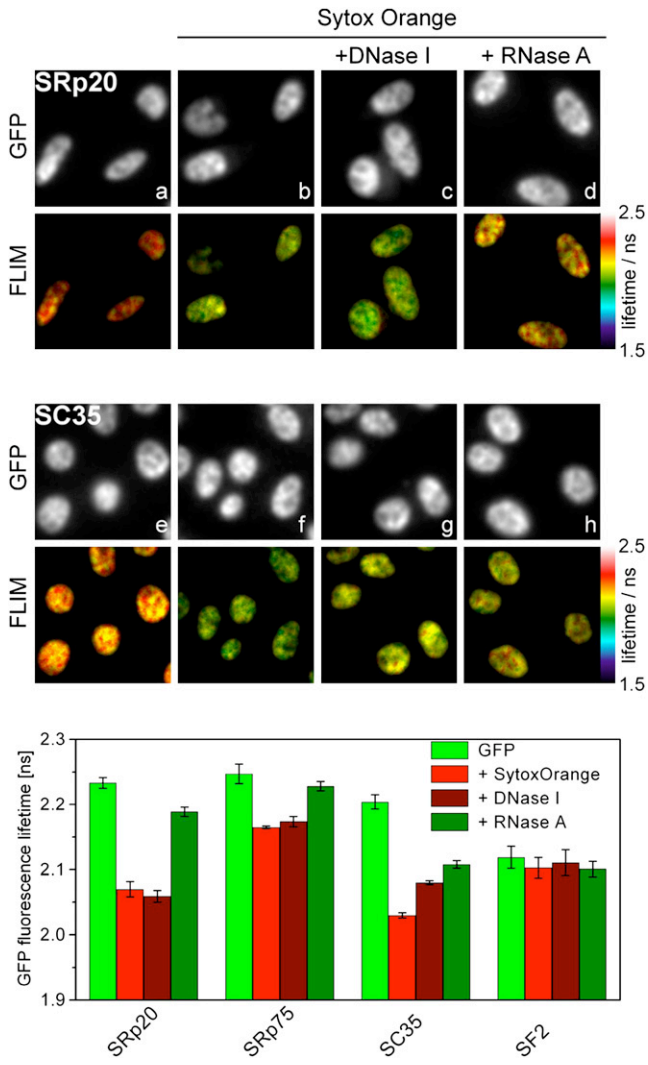

Figure 5. Measurement of FRET-FLIM between SR Proteins and RNA In Situ

(Upper panel) Grayscale images show GFP signals from two representative experiments, using stable cell lines expressing SRp20-GFP (A–D) and SC35-GFP (E–H). Fluorescence lifetimes of GFP were measured in the absence (A and E) or presence of 5 μM SytoxOrange (B and F). FRET between GFP tags and SytoxOrange is visible in the color panels as a decrease in the GFP fluorescence lifetime. In both samples, treatment with RNase A reduced FRET and led to an increase in fluorescence lifetime in the presence of SytoxOrange (A and H). Treatment with DNase I reduced FRET for SC35-GFP only (G). The first row shows the GFP fluorescence intensity images; the second row shows the lifetime images. (Lower panel) Corresponding GFP lifetime histograms for SRp20, SRp75, SC35, and SF2 plotted for indicated conditions. Note that SF2-GFP does not undergo FRET with SytoxOrange, yet provides a negative control, showing that RNase and DNase treatments do not alter FLIM measurements artifactually. The data represent measurements from n = 20–30 different cells, and the error bars are SEM.

U1-70K protein by western blot (Figure 6C). An association with U1-70K was detected for SF2; very weakly for SRp75; and not at all for SRp20, 9G8, SC35, or SRp55. Second, each cell line was metabolically labeled with P^{32} orthophosphate to interrogate all of the snRNAs in the pull-down. Although U1, U2, U4, U5, and U6 snRNAs were appropriately and well detected in the α-GFP pull-downs from Prp8-GFP or SmB-GFP cell lines, they were only weakly detected in the α-GFP pull-downs from the SR protein-GFP cell lines (Figure 6D). U1 snRNA was also recovered at low levels with SF2-GFP, SRp20-GFP, and SRp55-GFP as well as antibodies specific for endogenous SF2 (Figure S5), confirming the results in Figure 6C and showing that SF2-GFP behaves like the endogenous protein in this assay. This low level of snRNP association with SR proteins is expected, since SR proteins are detectable in spliceosomes (Makarov et al., 2002). Thus, SF2 interactions with the U1-70K protein were validated, but the association of SR proteins with snRNPs—and the U1 snRNP in particular—is not quantitative and cannot be generalized to all SR proteins.

If cotranscriptional association of SR proteins with active genes is independent of Pol II and snRNP binding, interrogation of individual SR protein activities on different genes should be possible. Therefore, the profiles of SRp20, 9G8, SC35, and SRp55 were examined by ChIP with qPCR of amplicons distributed along six genes selected for the following properties: *LDHA* and *PGK1* are highly transcribed and contain introns; Hsp70 (*HSPA1B*) and histone 2B (*HIST1H2AB*) are highly transcribed and intronless; and genes encoding fibronectin (*FN1*) and SRp20 (*SFRS3*) are alternatively spliced. The profiles of these SR proteins are significantly different from one another and do not strictly correlate with the presence of introns (Figure 7, Figure S4, and Table S1). Similar to the results on *FOS*, SR protein accumulation was not prominent at promoters where Pol II is concentrated, consistent with our conclusion (Figure 6) that SR proteins are not delivered to active genes by Pol II.

SRp20 and SC35 have been shown to regulate the alternative splicing of the *SFRS3* gene and are significantly detected on alternative exon 4 (Jumaa and Nielsen, 1997). Similarly, SRp55 and SC35 were significantly detected at gene positions corresponding to alternative exons EDA and EDB in *FN1*, but not on the exon downstream of EDB. Our HeLa cells include the EDB exon 50% of the time (data not shown), suggesting roles for SRp55 and SC35 in regulation of EDB. As SRp20 inhibits EDA inclusion and our cells always include EDA, the lack of SRp20 recruitment to EDA is expected (de la Mata and Kornblihtt, 2006). Although 9G8 is not detectable on EDA, SRp55 is; both of these SR proteins are reported to enhance inclusion (Buratti et al., 2004; Liang et al., 2007). Thus, the cotranscriptional accumulation of SR proteins on alternative exons correlates with splicing outcome.

To directly compare the gene targets studied by ChIP to later steps in gene expression, we probed the identity of the polyadenylated mRNAs stably associated with individual SR proteins. Indeed, widespread shuttling behavior suggests that SR proteins either escort cargo to the cytoplasm or associate de novo with new targets. Therefore, RNA immunoprecipitations (RIPs) were carried out with α-GFP for SRp20, 9G8, SRp55, and SC35, and nuclear and cytoplasmic fractions were compared (Figure 7). SRp20 and 9G8 showed a robust association with most of the RNAs assayed both in the nucleus and cytoplasm, in agreement with their high capacity for shuttling. Importantly, both SRp20 and 9G8 pulled down the endogenous *HIST1H2AB* RNA, the export of which was previously shown to require binding to these

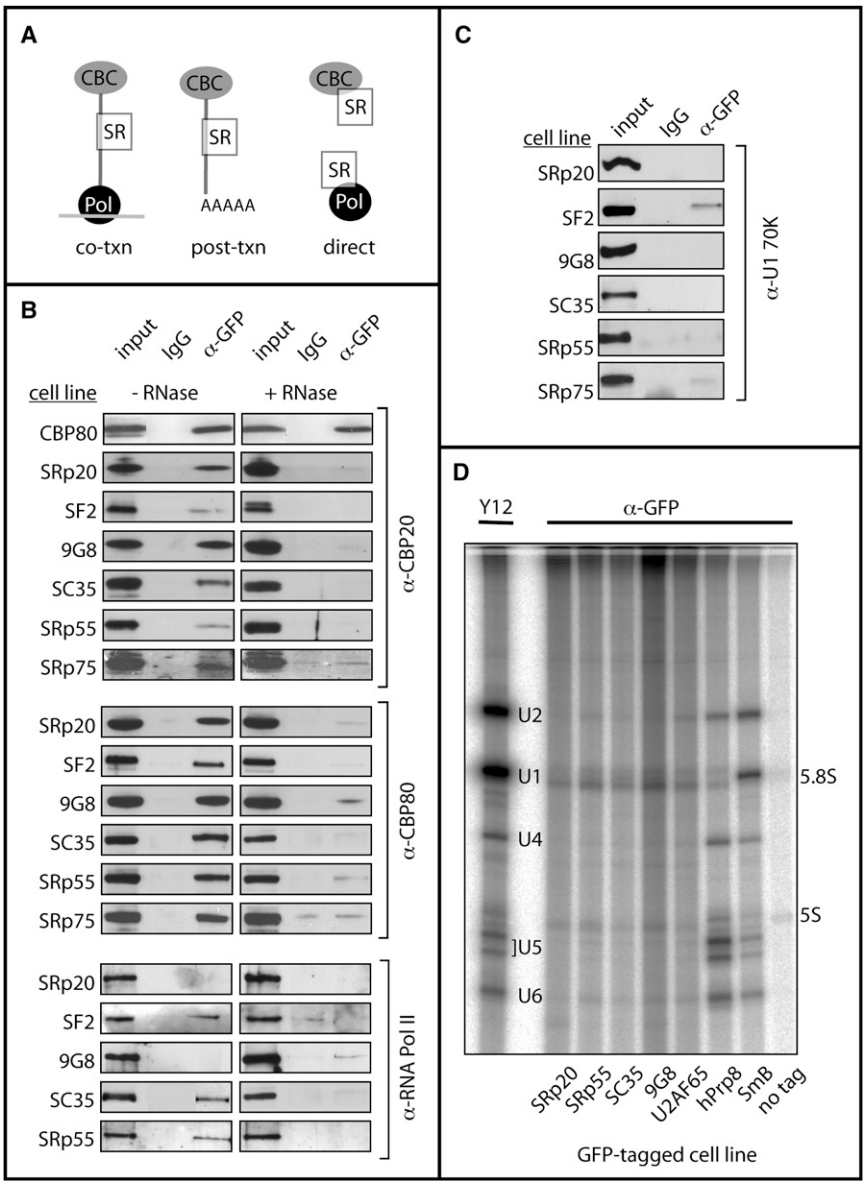

Figure 6. SR Protein Interactions with Nascent and Mature mRNPs

(A) Cartoon depicting possible interactions detectable in the coIP experiment: RNA-dependent interactions, both co- and posttranscriptional, and direct protein-protein interactions.

(B) CoIP was carried out with nonspecific IgG and α-GFP antibodies from RNase A-treated (+) or -untreated (–) extracts prepared from different GFP-tagged stable cell lines, as mentioned to the left of each panel. Inputs (1/100) and the IPs were analyzed by western blotting; specificities of the antibodies are indicated on the right side of each panel. These include α-CBP20, α-CBP80, and α-Pol II (mAbH5 specific for phosphorylated Ser2 of the CTD).

(C) CoIP of U1 snRNP with SR proteins was examined with α-U1-70K (mAb CB7).

(D) Metabolic labeling of snRNAs with P^{32} orthophosphate, followed by IP of the proteins indicated at the top of each lane. As a positive control, Prp8-GFP and SmB-GFP, compared with mAB Y12 against Sm proteins common to all snRNPs, show the expected composition of spliceosomal snRNPs, as indicated. The positions of each U snRNA, as well as contaminating 5S and 5.8S RNAs, are marked.

proteins (Huang and Steitz, 2001). Interestingly, neither of these SR proteins was detected cotranscriptionally on *HIST1H2AB*, indicating posttranscriptional recruitment. In contrast, SC35 was present on all the nuclear RNAs tested, consistent with the promiscuity detected cotranscriptionally. However, these associations did not persist in the cytoplasm, consistent with the observation that SC35 does not shuttle. Similarly, SRp55 bound to the SFRS3 gene and mRNA in the nucleus but was absent from cytoplasmic SFRS3 mRNPs, which were instead bound by SRp20 and 9G8. A comparison of RNA targets (Table S1) reveals the dynamic and differential behavior of SR proteins in vivo.

DISCUSSION

Here we have addressed the question of how SR proteins are recruited to active genes where they participate in nascent and mature RNP formation, including pre-mRNA splicing. To do so, we have introduced three technical advances, which allow us to gain access to a comprehensive set of SR proteins as they interact with nascent and mature RNA, chromatin, and RNA Pol II in vivo. These tools are (1) the use of BAC recombineering to generate a series of HeLa cell lines, expressing individual GFP-tagged SR proteins at physiological levels; (2) the application of splicing factor ChIP to GFP-tagged SR proteins, which can track the profile of SR protein family members along the length of genes; and (3) FRET/FLIM determinations of SR protein proximity to RNA and DNA in situ. Our data show that SR proteins interact primarily with RNA in living cells and that they are recruited to chromatin primarily via interactions with nascent RNA. Further experiments, showing the generality of nucleocytoplasmic shuttling for SR proteins as well as the continued association of SR proteins with mature mRNAs, strongly indicate the participation of SR proteins in gene expression, beyond their roles in splicing.

Each of the GFP-tagged SR proteins—SRp20, SF2, SC35, 9G8, SRp55, and SRp75—was detected by splicing factor ChIP on the active *FOS* gene. We conclude that accumulation of the SR protein family members is specified by interactions with the nascent RNA based on the following key observations. First, each SR protein was recruited to *FOS* in a transcription-dependent manner; no SR protein was detected on the

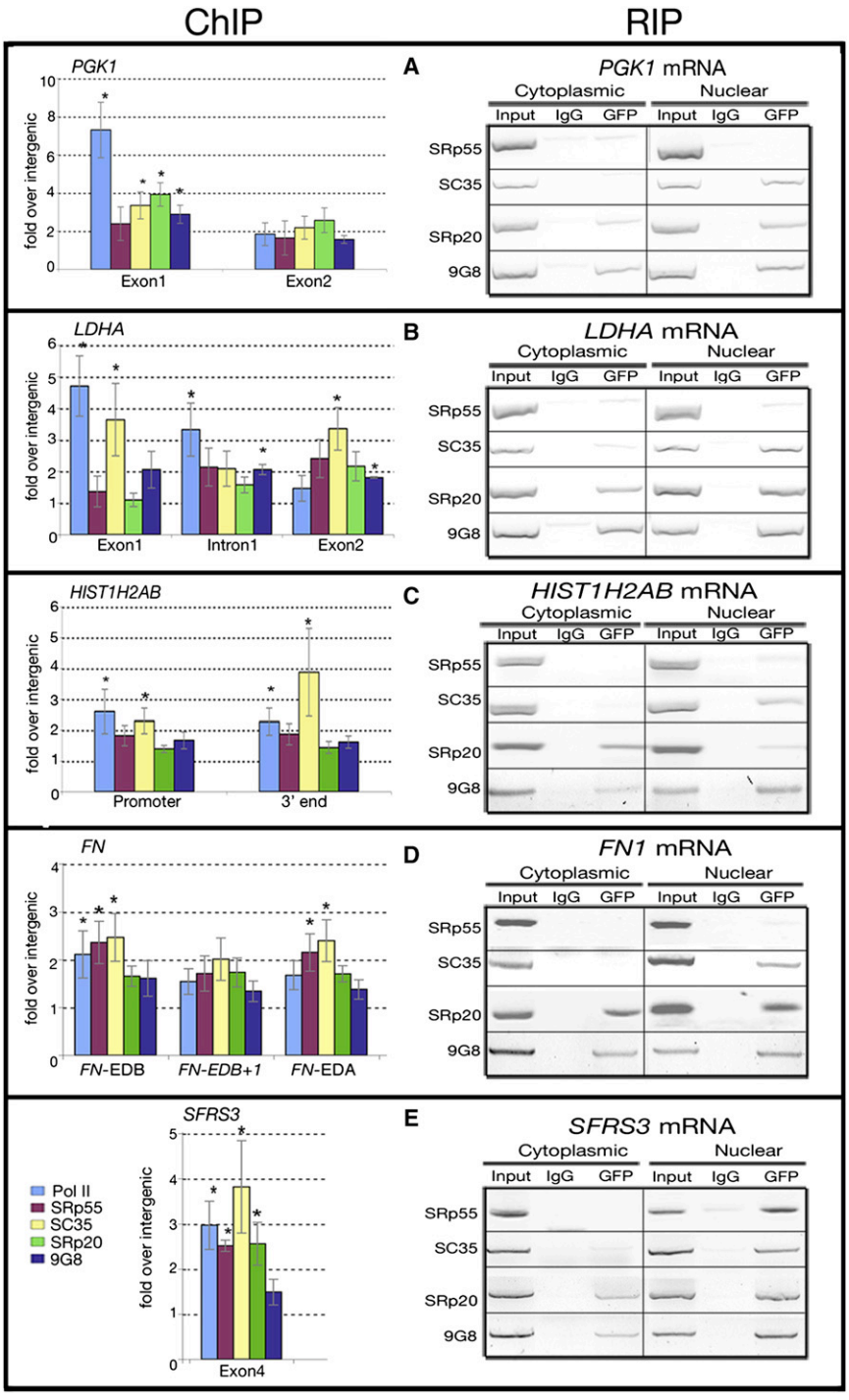

Figure 7. Comparison of Co- and Posttranscriptional RNA Targets of SR Proteins

(Left panel) ChIP profiles of Pol II and four GFP-tagged SR proteins on the indicated genes. (Right panel) RT-PCR analysis of RIPs carried out with these SR proteins from cytoplasmic or nuclear extracts. Assays were performed on intron-containing *PGK1* (A) and *LDHA* (B), intronless *HIST1H2AB* (C) as well as alternatively spliced *FN1* (D) and *SFRS3* (E). The y axis in the left panel denotes fold over intergenic. The x axis shows position within the transcript assayed for ChIP. Each data point represents the mean of four to seven biological replicates, error bars are SEM, and * denotes values significantly above background ($p < 0.05$). For RIP, equal amounts of extract were immunoprecipitated with α-GFP (for the tagged SR protein) or IgG (negative control). Input represents the RNA purified from 1/10 of the extract used. RNA purified from each IP was reverse transcribed, using oligo dT primers, except in the case of the histone message (C), for which gene-specific primers were used. cDNAs were then detected by PCR with gene-specific primers.

uninduced gene, even at the promoter where paused Pol II was robustly detectable (Figure 2); it is expected that SR proteins would be detected at the paused promoter if preassembled with Pol II by analogy to Pol II-bound capping factors (Glover-Cutter et al., 2008). Second, the SR proteins exhibited unique patterns of accumulation on *FOS*, which was attributed to the activity of the RRM domain (Figure 3). Third, SR protein detection on *FOS* was strongly sensitive to treatment of the crosslinked extract with RNase A (Figure 4). Fourth, apart from SC35, SR proteins were not robustly detectable on highly expressed intronless genes (Figure 7 and Figure S4). Fifth, the close proximity of SRp20, SRp75, and SC35 to RNA as detected by FRET/FLIM (Figure 5) underscores the likelihood that SR proteins are bound directly to RNA generally throughout the nucleus. Taken together, the behavior of SR proteins in vivo indicates dynamic interactions with nascent RNA rather than recruitment to chromatin through stable preassembly with Pol II.

A recent study, exploiting a coupled transcription and splicing assay in vitro, provided evidence that SR proteins couple splicing to transcription; key observations were the identification of SR proteins and the U1 snRNP in a mass spectrometry analysis of Pol II and the demonstration that SF2 pulls down U1 snRNP (Das et al., 2007). This led to the proposal that SR proteins are recruited to active genes by indirect binding to Pol II via interactions with U1 snRNP. However, a previous study failed to detect in vivo binding between U1 snRNP and Pol II, irrespective of the phosphorylation state of the CTD (Listerman et al., 2006). Here we investigated stable assemblies of SR proteins with Pol II—either direct or indirect—by coimmunoprecipitation. Our conditions permitted the detection of RNPs containing the CBC and mRNA, and we were able to verify the association of SF2 with U1 snRNP (Das

et al., 2007). However, Pol II was only weakly detected in pull-downs with individual SR proteins, and these interactions were RNase sensitive (Figure 6). We conclude that SR proteins bind more strongly in vivo to (pre-m)RNA than they do to either Pol II or the U1 snRNP. Thus, the interactions between SR proteins and Pol II are mediated by nascent RNA and are not due to the preassembly of the splicing factors with the transcriptional machinery. Consistent with this, U1 snRNP does not associate with intronless genes (Listerman et al., 2006), on which some SR proteins were detected in this study, indicating that SR proteins do not require snRNPs to bind nascent RNA. These results also agree with the absence of snRNPs and SR proteins from most purified Pol II complexes and, conversely, the absence of Pol II from purified spliceosomes (Jeronimo et al., 2007; Jurica et al., 2002; Makarov et al., 2002; Rappsilber et al., 2002; Tardiff et al., 2007; Zhou et al., 2002). However, because SR proteins in splicing extracts or in cells have been shown to contact Pol II, the U1 snRNP, and/or U2AF35 (Das et al., 2007; de la Mata and Kornblihtt, 2006; Du and Warren, 1997; Ellis et al., 2008; Kohtz et al., 1994; Misteli and Spector, 1999; Robert et al., 2002; Wu and Maniatis, 1993), we propose that these dynamic protein-protein associations reinforce the interaction of SR proteins with target RNAs.

The profiles of the different SR proteins on the endogenous genes examined reveal several general points about the cotranscriptional activities of SR proteins. First, SR proteins are recruited on constitutive as well as alternatively spliced transcripts, reiterating their role in both constitutive and alternative splicing regulation. Second, each SR protein accumulated on a distinct set of active genes. Unlike the other SR proteins examined, SC35 was present on all genes assayed. Because SC35 is a nonshuttling SR protein, its cotranscriptional recruitment must be explained by a solely nuclear function. Recent experiments indicate that SC35 plays a direct role in transcriptional elongation as well as genome stability (Lin et al., 2008; Xiao et al., 2007). This is consistent with the FRET interaction we detected between SC35 and DNA (see Figure 5); however, because SRp20 and SRp75 underwent FRET only with RNA, not DNA, we suggest that SC35 may be unique in this respect. Third, cotranscriptional accumulation was not predictive for SR protein association with mRNPs; for example, SRp20 was not cotranscriptionally recruited to the histone gene *HIST1H2AB* but was associated with the histone mRNP, likely reflecting its role in nuclear export of this mRNA (Huang and Steitz, 2001). However, some SR proteins may indeed be assembled into mRNPs during splicing and persist throughout export and translation activation (Merz et al., 2007; Sanford et al., 2008).

SR protein behaviors in nucleocytoplasmic shuttling as well as nuclear and cytoplasmic mRNP composition emphasize the potential for further roles after pre-mRNA splicing. SRp55 and SRp75 belong to the class of SR proteins that undergo nucleocytoplasmic shuttling, along with SF2, SRp20, and 9G8 (Caceres et al., 1998; Hautbergue et al., 2008; Huang and Steitz, 2001). We conclude that nucleocytoplasmic shuttling is the norm for SR proteins, with SC35 being an exception. Consistent with this, analysis of mRNAs associated with individual SR proteins revealed that SC35 could not be detected in any cytoplasmic mRNP tested, while SRp20, 9G8, and SRp55 were. In view of this, it would be of future interest to investigate the role of these shuttling SR proteins in the integration of cellular signaling programs that can modulate splicing and translation through regulated phosphorylation of the RS domain (Blaustein et al., 2005; Sanford et al., 2005). Following on the discoveries that SRp20, 9G8, and SF2 have activities in mRNA export and/or translation, our data confirm that the SR proteins play widespread roles in the cytoplasmic life of mRNPs.

The unique behavior of SR proteins with respect to cotranscriptional gene associations, binding patterns within target genes, differences in nucleocytoplasmic shuttling activities, and differential association with mature mRNPs combine to support essential roles for each member of the SR protein family in gene expression. An interesting possibility is that SR protein association with nascent RNA contributes to the structure and function of the mRNP emerging at the transcription site. For example, the observation that intron continuity is not required for splicing implies that nascent RNA is held together by the forming RNP and perhaps stabilized by low-affinity interactions with Pol II (Dye et al., 2006). Because SR proteins have been shown to link exons together across introns, their ordered assembly with nascent RNA may accomplish this function and further influence splice site selection (Neugebauer, 2006; Stark et al., 1998). Such dynamic roles for members of the SR protein family in the formation of nascent and mature mRNPs are now accessible to further exploration.

EXPERIMENTAL PROCEDURES

Cell Culture and Treatments

HeLa cells were grown in DMEM supplemented with 100 U/ml penicillin, 100 μg/ml streptomycin, and 10% FBS. Stable cell lines expressing the recombineered BACs were generated by transfection of HeLa cells with Effectene (QIAGEN) and selection with 0.4–1 mg/ml Geneticin. Constructs for transient transfection were generated in pEGFP-N1 (Clontech) and sequenced; transfections were carried out with Fugene and assayed after 48 hr. To induce *FOS*, cells were serum starved for 2 hr and then treated with 5 μM calcium ionophore (A23187, Sigma) for 15 min. For *HSPA1B* induction, cells were treated with 250 μM sodium (meta)arsenite (Sigma) for 1 hr. Cells were subjected to cadmium stress as described (Denegri et al., 2001).

BAC Tagging

BACs were ordered from BACPAC Resources Center (http://bacpac.chori.org). The EGFP-IRES-Neo or LAP-IRES-Neo cassette was PCR amplified with primers carrying 50 nt of homology to the targeted sequence. Recombineering of the BACs with the PCR product was performed as described (Poser et al., 2008; Zhang et al., 1998).

Antibodies

Goat α-GFP polyclonal antibodies were the kind gift of David Drechsel and used at 12 μg/IP. Monoclonal antibodies used against Pol II were H5 (a gift of Y. Shav-Tal), 4H8 (Abcam), and Pol3/3 against the F domain of Pol II (gift of D. Eick). Other antibodies include monoclonal antibody CB7 against U1-70K (gift of D.L. Black), MC3 against U2AF65 (gift of M. Carmo-Fonseca), mAB 104 against the family of SR proteins, AK103 and AK96 against SF2 (Zymed), α-SRp20 (Neugebauer and Roth, 1997), polyclonal antibodies against CBP80 and CBP20 (gift of E. Izaurralde), 9G8 and α-SC35 (gift of J. Stevenin), and α-HAP (gift of G. Biamonti).

ChIP and qPCR

ChIP and real-time PCR protocols were according to Listerman et al. (2006). Extract from 10^8 HeLa cells was used per ChIP. For RNase-treated extracts, crosslinked, washed cell pellets were resuspended in 0.1% SDS lysis buffer, sonicated and treated with 400 μg/ml of RNase A at 37°C for 20 min. The

samples were then centrifuged at 20,000 × g for 10 min before proceeding with the supernatant for preclearing and IP. ChIP data are represented after normalization to the nonimmune control and as fold enrichment above an intergenic region on chromosome 10 lacking annotated genes. Primer sequences used in the qPCR analysis can be obtained on request.

RNA Immunoprecipitation

RIPs were carried out from uncrosslinked extracts prepared according to Mili et al. (2001). Briefly, 10^8 cells were washed in cold PBS and then resuspended in 1 ml of RSB-100 buffer (10 mM Tris-HCl [pH 7.4], 100 mM NaCl, 2.5 mM $MgCl_2$) containing 40 μg/ml digitonin. After incubating for 5 min, samples were spun at 2000 × g for 8 min. The supernatant was considered the cytoplasmic fraction. The pellet was resuspended in 1 ml RSB-100 buffer containing 40 μg/ml digitonin and 0.5% (v/v) Triton X-100 and incubated for 10 min on ice. Samples were spun at 2000 × g for 8 min, and the supernatant represented the soluble nuclear fraction. The 1 ml extracts were split and immunoprecipitated with either nonspecific IgG or α-GFP. Beads were washed with RSB-100 with 0.05% NP40, resuspended in 300 μl of the wash buffer supplemented with 20 μg tRNA and 1% SDS, and then extracted in an equal volume of phenol/chloroform at 37°C for 1 hr. Following ethanol precipitation, the RNA pellet was used in a 20 μl RT-PCR reaction with Invitrogen Superscript III reverse transcriptase, using oligo dT or HISTH2AB-specific reverse primers. One microliter of the reaction was used in a normal PCR reaction to assay for the presence of specific mRNAs.

Immunoprecipitations and Western Blot Analysis

Whole-cell extract from ~10^8 HeLa cells was prepared in NET-2 buffer (50 mM Tris-HCl [pH 7.5], 150 mM NaCl, 0.05% NP40) containing protease inhibitors (Roche). Half the extract was treated with RNase A, 400 μg/ml, at 37°C for 20 min. IPs were carried out at 4°C for 3 hr, using α-GFP and blocked GammaBind G Sepahrose (GE Healthcare). Beads were washed four times with NET-2 buffer. The immunoprecipitate was resolved on a 4%–12% gradient gel and analyzed by western blot analysis for coimmunoprecipitation (coIP) of proteins of interest. Metabolic labeling was carried out by incubating 15 cm dishes in phosphate-free medium + 1%FCS and 100 μCi ^{32}P-orthophosphate overnight, followed by lysis and IP with α-Sm (Y12) or α-GFP. RNA was extracted from the final pellets with phenol/chloroform, precipitated, resolved on a 10% urea gel, and analyzed by PhosphorImager.

Heterokaryon Assay

Stably transfected HeLa cells were seeded on coverslips and incubated overnight. Equal numbers of NIH 3T3 cells were added and cocultured in 50 μg/ml cycloheximide (CHX, Sigma) for 1 hr, as described (Caceres et al., 1998). CHX was raised to 100 μg/ml for 30 min, followed by cell fusion with PEG1500 (Roche) and incubation for 4 hr in the presence of 100 μg/ml CHX. After fixation with 4% PFA, cells were incubated with 1 μg/ml Hoechst 33258 (Sigma) and mounted. Images were acquired with Zeiss Axioplan 2 MOT microscope coupled to a CCD camera.

FRET/FLIM Assay

Stably transfected HeLa cell lines were fixed for 10 min in 4% formaldehyde at 37°C. Following permeabilization with PBS containing 0.5% Triton X-100, excess aldehyde groups were blocked with 100 mM glycine for 10 min at RT. Nucleic acids were digested either with 0.1 mg/ml RNase A (Roche Diagnostics) in PBS or 20 U/ml DNase I (New England BioLabs) in DNase I buffer for 30 min at 37°C, respectively. Finally, cells were stained with 5 μM SytoxOrange (Molecular Probes) in TAE buffer for 20 min, washed, and mounted with ProLong Gold antifade (Molecular Probes) or Vectashield (Linaris, Germany). Briefly, GFP was excited at 488 nm with a Chameleon XR Ti:Sapphire Laser (Coherent) tuned at 976 nm. A detailed description of the FLIM instrument, lifetime measurements, and analyzes can be found elsewhere (Lorenz, 2009).

SUPPLEMENTAL DATA

The Supplemental Data include five figures and one table and can be found with this article online at http://www.cell.com/molecular-cell/supplemental/S1097-2765(09)00147-6.

ACKNOWLEDGMENTS

We are grateful to I. Listerman for her early involvement in the project and comments on the manuscript. L. Morales, J. Görnemann, M. Strzelecka, and F. Carillo-Oesterreich also provided valuable insights. We thank J. Stevenin, D. Eick, E. Izuarralde, M. Carmo-Fonseca, D. Black, Y. Shav-Tal, and G. Biamonti for generous gifts of antibodies. We thank the Hyman and Buchholz labs for sharing BAC technology and M. Augsburg for help establishing the SF2- and U1-70K-tagged cell lines (with funding from Mitocheck). This work was directly supported by a Marie Curie Fellowship (to A.K.S.), a Sigrid Juselius fellowship (to M.-L.A.), the Max Planck Society, and EURASNET (FP6 Network of Excellence to K.M.N.).

Received: October 8, 2008
Revised: December 19, 2008
Accepted: February 25, 2009
Published: April 23, 2009

REFERENCES

Batsche, E., Yaniv, M., and Muchardt, C. (2006). The human SWI/SNF subunit Brm is a regulator of alternative splicing. Nat. Struct. Mol. Biol. *13*, 22–29.

Blaustein, M., Pelisch, F., Tanos, T., Munoz, M.J., Wengier, D., Quadrana, L., Sanford, J.R., Muschietti, J.P., Kornblihtt, A.R., Caceres, J.F., et al. (2005). Concerted regulation of nuclear and cytoplasmic activities of SR proteins by AKT. Nat. Struct. Mol. Biol. *12*, 1037–1044.

Blencowe, B.J. (2006). Alternative splicing: new insights from global analyses. Cell *126*, 37–47.

Buratti, E., Muro, A.F., Giombi, M., Gherbassi, D., Iaconcig, A., and Baralle, F.E. (2004). RNA folding affects the recruitment of SR proteins by mouse and human polypurinic enhancer elements in the fibronectin EDA exon. Mol. Cell. Biol. *24*, 1387–1400.

Caceres, J.F., Stamm, S., Helfman, D.M., and Krainer, A.R. (1994). Regulation of alternative splicing in vivo by overexpression of antagonistic splicing factors. Science *265*, 1706–1709.

Caceres, J.F., Screaton, G.R., and Krainer, A.R. (1998). A specific subset of SR proteins shuttles continuously between the nucleus and the cytoplasm. Genes Dev. *12*, 55–66.

Das, R., Dufu, K., Romney, B., Feldt, M., Elenko, M., and Reed, R. (2006). Functional coupling of RNAP II transcription to spliceosome assembly. Genes Dev. *20*, 1100–1109.

Das, R., Yu, J., Zhang, Z., Gygi, M.P., Krainer, A.R., Gygi, S.P., and Reed, R. (2007). SR proteins function in coupling RNAP II transcription to pre-mRNA splicing. Mol. Cell *26*, 867–881.

de la Mata, M., and Kornblihtt, A.R. (2006). RNA polymerase II C-terminal domain mediates regulation of alternative splicing by SRp20. Nat. Struct. Mol. Biol. *13*, 973–980.

de la Mata, M., Alonso, C.R., Kadener, S., Fededa, J.P., Blaustein, M., Pelisch, F., Cramer, P., Bentley, D., and Kornblihtt, A.R. (2003). A slow RNA polymerase II affects alternative splicing in vivo. Mol. Cell *12*, 525–532.

Denegri, M., Chiodi, I., Corioni, M., Cobianchi, F., Riva, S., and Biamonti, G. (2001). Stress-induced nuclear bodies are sites of accumulation of pre-mRNA processing factors. Mol. Biol. Cell *12*, 3502–3514.

Du, L., and Warren, S.L. (1997). A functional interaction between the carboxy-terminal domain of RNA polymerase II and pre-mRNA splicing. J. Cell Biol. *136*, 5–18.

Dye, M.J., Gromak, N., and Proudfoot, N.J. (2006). Exon Tethering in Transcription by RNA Polymerase II. Mol. Cell *21*, 849–859.

Ellis, J.D., Lleres, D., Denegri, M., Lamond, A.I., and Caceres, J.F. (2008). Spatial mapping of splicing factor complexes involved in exon and intron definition. J. Cell Biol. *181*, 921–934.

Fu, X.D., and Maniatis, T. (1990). Factor required for mammalian spliceosome assembly is localized to discrete regions in the nucleus. Nature *343*, 437–441.

Gama-Carvalho, M., Carvalho, M.P., Kehlenbach, A., Valcarcel, J., and Carmo-Fonseca, M. (2001). Nucleocytoplasmic shuttling of heterodimeric splicing factor U2AF. J. Biol. Chem. *276*, 13104–13112.

Ge, H., and Manley, J.L. (1990). A protein factor, ASF, controls cell-specific alternative splicing of SV40 early pre-mRNA in vitro. Cell *62*, 25–34.

Ghosh, S., and Garcia-Blanco, M.A. (2000). Coupled in vitro synthesis and splicing of RNA polymerase II transcripts. RNA *6*, 1325–1334.

Glover-Cutter, K., Kim, S., Espinosa, J., and Bentley, D.L. (2008). RNA polymerase II pauses and associates with pre-mRNA processing factors at both ends of genes. Nat. Struct. Mol. Biol. *15*, 71–78.

Gornemann, J., Kotovic, K.M., Hujer, K., and Neugebauer, K.M. (2005). Cotranscriptional spliceosome assembly occurs in a stepwise fashion and requires the cap binding complex. Mol. Cell *19*, 53–63.

Hautbergue, G.M., Hung, M.L., Golovanov, A.P., Lian, L.Y., and Wilson, S.A. (2008). Mutually exclusive interactions drive handover of mRNA from export adaptors to TAP. Proc. Natl. Acad. Sci. USA *105*, 5154–5159.

Hertel, K.J. (2008). Combinatorial control of exon recognition. J. Biol. Chem. *283*, 1211–1215.

Hicks, M.J., Yang, C.R., Kotlajich, M.V., and Hertel, K.J. (2006). Linking splicing to Pol II transcription stabilizes pre-mRNAs and influences splicing patterns. PLoS Biol. *4*, e147. 10.1371/journal.pbio.0040147.

Huang, Y., and Steitz, J.A. (2001). Splicing factors SRp20 and 9G8 promote the nucleocytoplasmic export of mRNA. Mol. Cell *7*, 899–905.

Huang, Y., Gattoni, R., Stevenin, J., and Steitz, J.A. (2003). SR splicing factors serve as adapter proteins for TAP-dependent mRNA export. Mol. Cell *11*, 837–843.

Jeronimo, C., Forget, D., Bouchard, A., Li, Q., Chua, G., Poitras, C., Therien, C., Bergeron, D., Bourassa, S., Greenblatt, J., et al. (2007). Systematic analysis of the protein interaction network for the human transcription machinery reveals the identity of the 7SK capping enzyme. Mol. Cell *27*, 262–274.

Jumaa, H., and Nielsen, P.J. (1997). The splicing factor SRp20 modifies splicing of its own mRNA and ASF/SF2 antagonizes this regulation. EMBO J. *16*, 5077–5085.

Jurica, M.S., Licklider, L.J., Gygi, S.R., Grigorieff, N., and Moore, M.J. (2002). Purification and characterization of native spliceosomes suitable for three-dimensional structural analysis. RNA *8*, 426–439.

Karni, R., de Stanchina, E., Lowe, S.W., Sinha, R., Mu, D., and Krainer, A.R. (2007). The gene encoding the splicing factor SF2/ASF is a proto-oncogene. Nat. Struct. Mol. Biol. *14*, 185–193.

Kohtz, J.D., Jamison, S.F., Will, C.L., Zuo, P., Luhrmann, R., Garcia-Blanco, M.A., and Manley, J.L. (1994). Protein-protein interactions and 5′-splice-site recognition in mammalian mRNA precursors. Nature *368*, 119–124.

Kornblihtt, A.R. (2006). Chromatin, transcript elongation and alternative splicing. Nat. Struct. Mol. Biol. *13*, 5–7.

Krainer, A.R., Conway, G.C., and Kozak, D. (1990). Purification and characterization of pre-mRNA splicing factor SF2 from HeLa cells. Genes Dev. *4*, 1158–1171.

Lacadie, S.A., and Rosbash, M. (2005). Cotranscriptional spliceosome assembly dynamics and the role of U1 snRNA:5′ss base pairing in yeast. Mol. Cell *19*, 65–75.

Lamond, A.I., and Spector, D.L. (2003). Nuclear speckles: a model for nuclear organelles. Nat. Rev. Mol. Cell Biol. *4*, 605–612.

Lazarev, D., and Manley, J.L. (2007). Concurrent splicing and transcription are not sufficient to enhance splicing efficiency. RNA *13*, 1546–1557.

Lewis, J.D., and Tollervey, D. (2000). Like attracts like: getting RNA processing together in the nucleus. Science *288*, 1385–1389.

Li, X., and Manley, J.L. (2005). Inactivation of the SR protein splicing factor ASF/SF2 results in genomic instability. Cell *122*, 365–378.

Li, X., Wang, J., and Manley, J.L. (2005). Loss of splicing factor ASF/SF2 induces G2 cell cycle arrest and apoptosis, but inhibits internucleosomal DNA fragmentation. Genes Dev. *19*, 2705–2714.

Liang, H., Tuan, R.S., and Norton, P.A. (2007). Overexpression of SR proteins and splice variants modulates chondrogenesis. Exp. Cell Res. *313*, 1509–1517.

Lin, S., and Fu, X.D. (2007). SR proteins and related factors in alternative splicing. Adv. Exp. Med. Biol. *623*, 107–122.

Lin, S., Coutinho-Mansfield, G., Wang, D., Pandit, S., and Fu, X.D. (2008). The splicing factor SC35 has an active role in transcriptional elongation. Nat. Struct. Mol. Biol. *15*, 819–826.

Listerman, I., Sapra, A.K., and Neugebauer, K.M. (2006). Cotranscriptional coupling of splicing factor recruitment and precursor messenger RNA splicing in mammalian cells. Nat. Struct. Mol. Biol. *13*, 815–822.

Lorenz, M. (2009). Visualizing protein-RNA interactions inside cells by fluorescence resonance energy transfer. RNA *15*, 97–103.

Mabon, S.A., and Misteli, T. (2005). Differential recruitment of pre-mRNA splicing factors to alternatively spliced transcripts in vivo. PLoS Biol. *3*, e374. 10.1371/journal.pbio.0030374.

Makarov, E.M., Makarova, O.V., Urlaub, H., Gentzel, M., Will, C.L., Wilm, M., and Luhrmann, R. (2002). Small nuclear ribonucleoprotein remodeling during catalytic activation of the spliceosome. Science *298*, 2205–2208.

Matlin, A.J., Clark, F., and Smith, C.W. (2005). Understanding alternative splicing: towards a cellular code. Nat. Rev. Mol. Cell Biol. *6*, 386–398.

Merz, C., Urlaub, H., Will, C.L., and Luhrmann, R. (2007). Protein composition of human mRNPs spliced in vitro and differential requirements for mRNP protein recruitment. RNA *13*, 116–128.

Mili, S., Shu, H.J., Zhao, Y., and Pinol-Roma, S. (2001). Distinct RNP complexes of shuttling hnRNP proteins with pre-mRNA and mRNA: candidate intermediates in formation and export of mRNA. Mol. Cell. Biol. *21*, 7307–7319.

Misteli, T., and Spector, D.L. (1999). RNA polymerase II targets pre-mRNA splicing factors to transcription sites in vivo. Mol. Cell *3*, 697–705.

Misteli, T., Caceres, J.F., and Spector, D.L. (1997). The dynamics of a pre-mRNA splicing factor in living cells. Nature *387*, 523–527.

Moore, M.J., and Proudfoot, N.J. (2009). Pre-mRNA processing reaches back to transcription and ahead to translation. Cell *136*, 688–700.

Natalizio, B.J., Robson-Dixon, N.D., and Garcia-Blanco, M.A. (2009). The carboxyl-terminal domain of RNA polymerase II is not sufficient to enhance the efficiency of pre-mRNA capping or splicing in the context of a different polymerase. J. Biol. Chem. *284*, 8692–8702.

Neugebauer, K.M. (2002). On the importance of being co-transcriptional. J. Cell Sci. *115*, 3865–3871.

Neugebauer, K.M. (2006). Please hold—the next available exon will be right with you. Nat. Struct. Mol. Biol. *13*, 385–386.

Neugebauer, K.M., and Roth, M.B. (1997). Distribution of pre-mRNA splicing factors at sites of RNA polymerase II transcription. Genes Dev. *11*, 1148–1159.

Poser, I., Sarov, M., Hutchins, J.R., Heriche, J.K., Toyoda, Y., Pozniakovsky, A., Weigl, D., Nitzsche, A., Hegemann, B., Bird, A.W., et al. (2008). BAC TransgeneOmics: a high-throughput method for exploration of protein function in mammals. Nat. Methods *5*, 409–415.

Rappsilber, J., Ryder, U., Lamond, A.I., and Mann, M. (2002). Large-scale proteomic analysis of the human spliceosome. Genome Res. *12*, 1231–1245.

Robert, F., Blanchette, M., Maes, O., Chabot, B., and Coulombe, B. (2002). A human RNA polymerase II-containing complex associated with factors necessary for spliceosome assembly. J. Biol. Chem. *277*, 9302–9306.

Sanford, J.R., Gray, N.K., Beckmann, K., and Caceres, J.F. (2004). A novel role for shuttling SR proteins in mRNA translation. Genes Dev. *18*, 755–768.

Sanford, J.R., Ellis, J.D., Cazalla, D., and Caceres, J.F. (2005). Reversible phosphorylation differentially affects nuclear and cytoplasmic functions of splicing factor 2/alternative splicing factor. Proc. Natl. Acad. Sci. USA *102*, 15042–15047.

Sanford, J.R., Coutinho, P., Hackett, J.A., Wang, X., Ranahan, W., and Caceres, J.F. (2008). Identification of nuclear and cytoplasmic mRNA targets for the shuttling protein SF2/ASF. PLoS ONE *3*, e3369. 10.1371/journal.pone.0003369.

Shen, H., and Green, M.R. (2006). RS domains contact splicing signals and promote splicing by a common mechanism in yeast through humans. Genes Dev. *20*, 1755–1765.

Shen, H., Kan, J.L., and Green, M.R. (2004). Arginine-serine-rich domains bound at splicing enhancers contact the branchpoint to promote prespliceosome assembly. Mol. Cell *13*, 367–376.

Stark, J.M., Bazett-Jones, D.P., Herfort, M., and Roth, M.B. (1998). SR proteins are sufficient for exon bridging across an intron. Proc. Natl. Acad. Sci. USA *95*, 2163–2168.

Tardiff, D.F., Abruzzi, K.C., and Rosbash, M. (2007). Protein characterization of Saccharomyces cerevisiae RNA polymerase II after in vivo cross-linking. Proc. Natl. Acad. Sci. USA *104*, 19948–19953.

Wahl, M.C., Will, C.L., and Lührmann, R. (2009). The spliceosome: design principles of a dynamic RNP machine. Cell *136*, 701–718.

Wang, J., and Manley, J.L. (1995). Overexpression of the SR proteins ASF/SF2 and SC35 influences alternative splicing in vivo in diverse ways. RNA *1*, 335–346.

Wang, J., Smith, P.J., Krainer, A.R., and Zhang, M.Q. (2005). Distribution of SR protein exonic splicing enhancer motifs in human protein-coding genes. Nucleic Acids Res. *33*, 5053–5062.

Wu, J.Y., and Maniatis, T. (1993). Specific interactions between proteins implicated in splice site selection and regulated alternative splicing. Cell *75*, 1061–1070.

Xiao, R., Sun, Y., Ding, J.H., Lin, S., Rose, D.W., Rosenfeld, M.G., Fu, X.D., and Li, X. (2007). Splicing regulator SC35 is essential for genomic stability and cell proliferation during mammalian organogenesis. Mol. Cell. Biol. *27*, 5393–5402.

Zahler, A.M., Lane, W.S., Stolk, J.A., and Roth, M.B. (1992). SR proteins: a conserved family of pre-mRNA splicing factors. Genes Dev. *6*, 837–847.

Zhang, Y., Buchholz, F., Muyrers, J.P., and Stewart, A.F. (1998). A new logic for DNA engineering using recombination in Escherichia coli. Nat. Genet. *20*, 123–128.

Zhou, Z., Licklider, L.J., Gygi, S.P., and Reed, R. (2002). Comprehensive proteomic analysis of the human spliceosome. Nature *419*, 182–185.

Molecular Cell, Volume *34*

Supplemental Data

SR Protein Family Members

Display Diverse Activities in the Formation

of Nascent and Mature mRNPs In Vivo

Aparna K. Sapra, Minna-Liisa Änkö, Inna Grishina, Mike Lorenz, Marta Pabis, Ina Poser, Jarod Rollins, Eva-Maria Weiland, and Karla M. Neugebauer

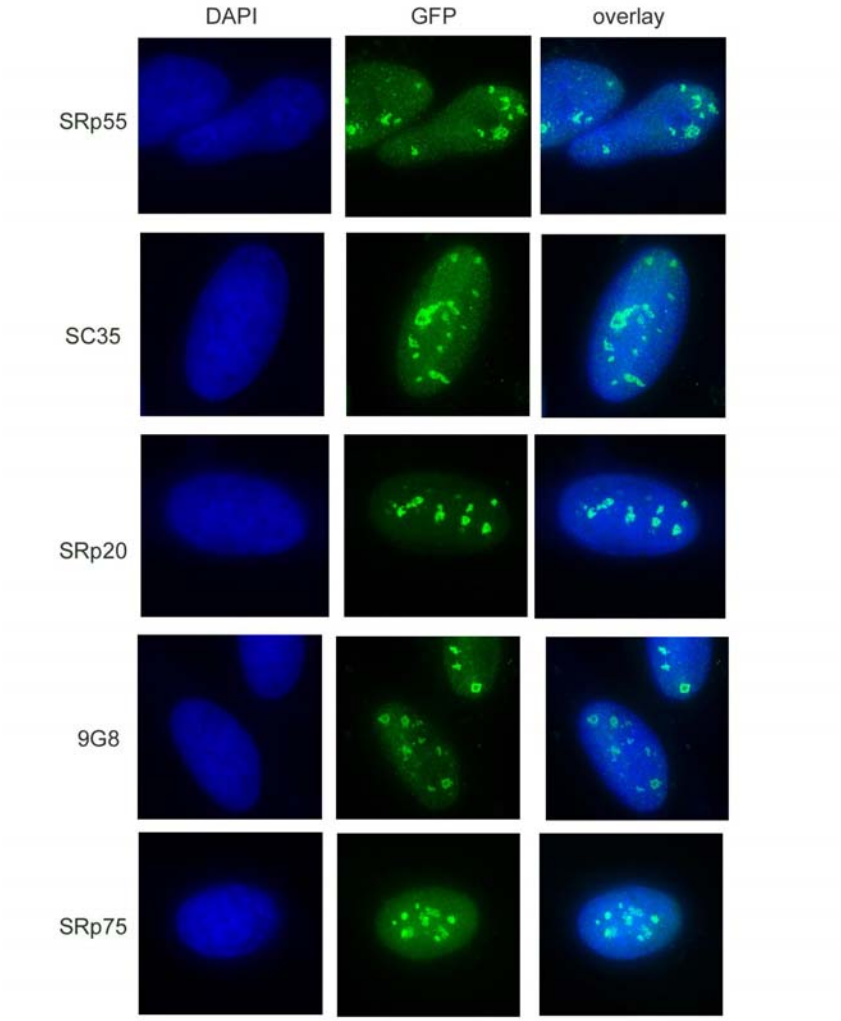

Figure S1. SR protein redistribution in response to α-amanitin treatment. Stable HeLa cells expressing GFP tagged SR proteins, U2AF65 or Prp8 were treated overnight with 10 μg/ml α-amanitin and observed for altered localization of the proteins. As expected, all SR proteins redistributed into rounded-up speckles.

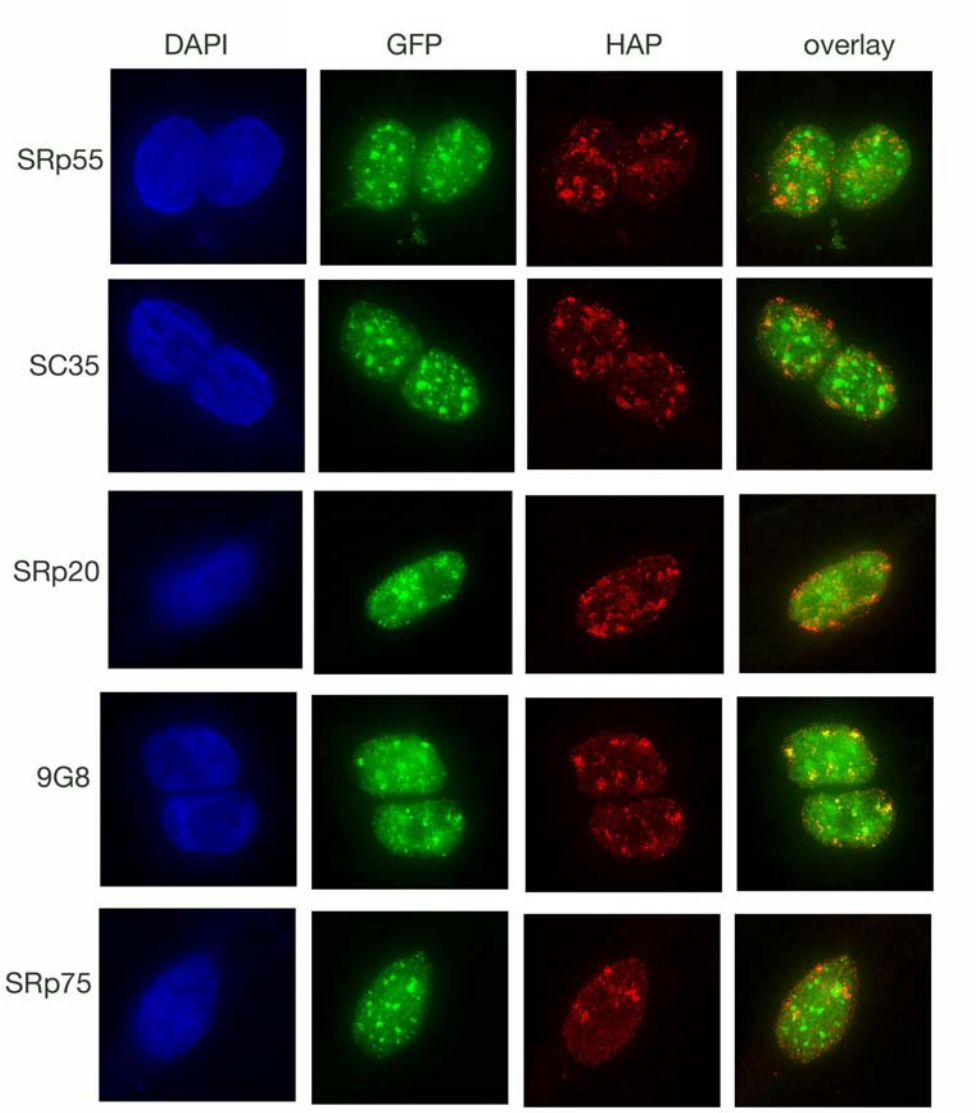

Figure S2. SR protein localization to stress bodies. Stable HeLa cells expressing GFP tagged SRp55, SC35, SRp20, 9G8 or SRp75 were stressed with CdSO4, leading to formation of nuclear stress bodies (nSBs) at the transcriptionally activated SATIII locus. The nSBs were marked by immunostaining with α-HAP antibody. The overlay between the red and green channels shows that 9G8 is enriched in nSBs, as expected, and that no other SR proteins tested accumulate detectably in nSBs. This indicates that SATIII RNA selectively recruits 9G8, as previously published (Denegri et al. 2001. Mol Biol. Cell. 12: 3502).

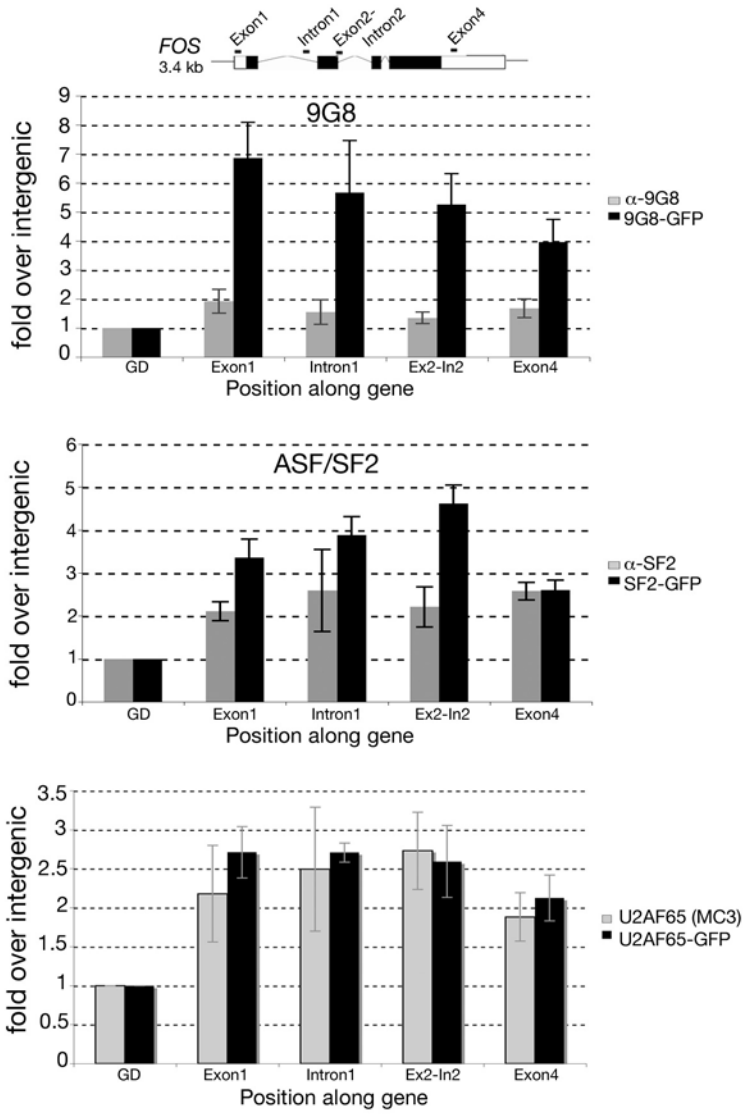

Figure S3. Comparison of ChIP profiles of endogenous and tagged proteins. ChIP profiles on c-*FOS* for 9G8, SF2 and U2AF65 were obtained for the endogenous protein by using specific antibodies (grey bars) and compared with profiles of the GFP tagged protein (black bars). Mean +/- SEM is shown for n=3 biological replicates.

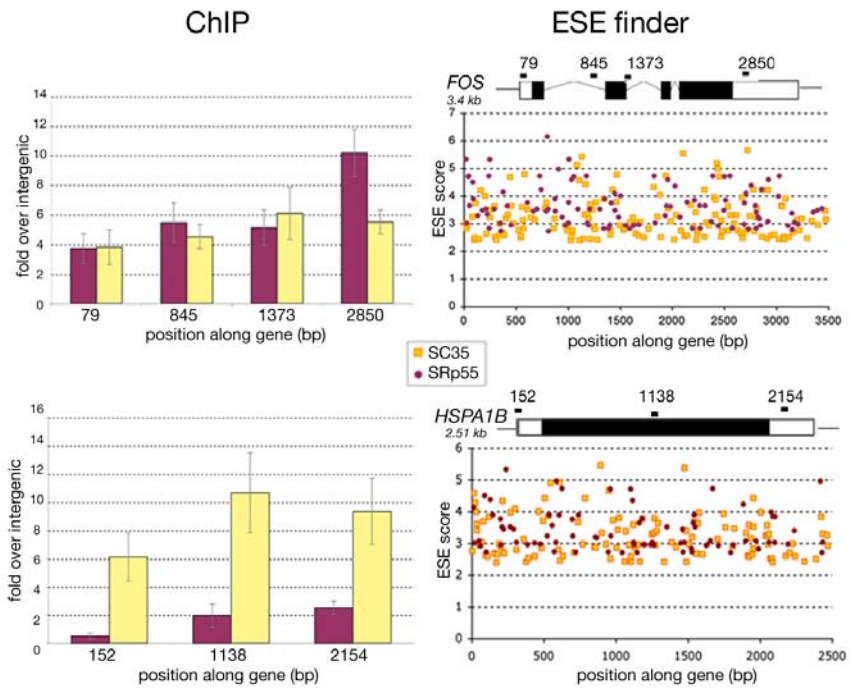

Figure S4. ESE and ChIP profiles for SC35 and SRp55 on *c-FOS* and *HSPA1B*. Left panels respresent co-transcriptional recruitment profiles of SC35 and SRp55 on c-*FOS* (top) and *HSPA1B* (bottom) by ChIP. Sequences for these transcripts were analysed using ESE finder 3.0 and ESE scores were derived using the default thresholds. The scores have been plotted along the gene length (Right panels). Positions of amplicons assayed using ChIP are marked in bp on the respective gene cartoon.

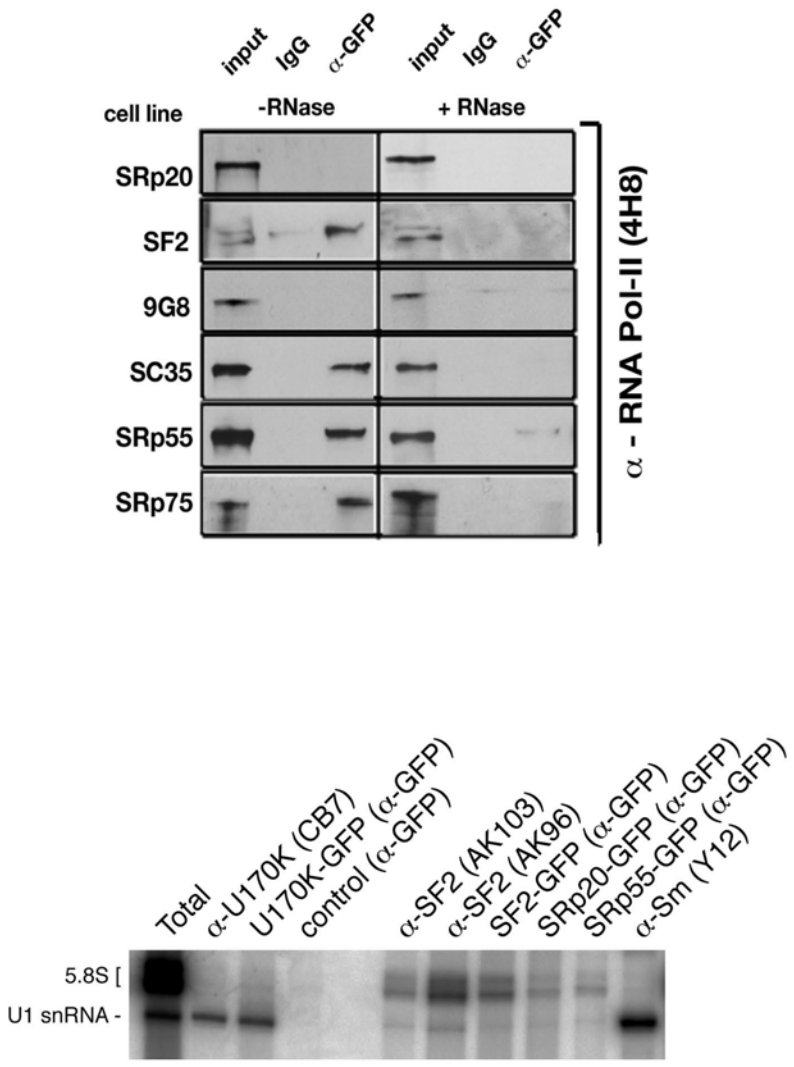

Figure S5. Co-immunoprecipiation of GFP-tagged SR proteins with Pol II and U1 snRNA. Top panel, co-IP of Pol II as detected by Western blot with monoclonal antibody 4H8, which binds Pol II independently of CTD phosphorylation state. Consistent with results in Fig 6C, Pol II is only detected in co-IP with a subset of SR proteins and these are fully RNase-sensitive. Lower panel, metabolic labeling with 32P-orthophosphate, followed by IP with either anti-GFP – pulling down different tagged SR proteins – or antibodies specific for endogenous SF2. Resolution of the isolated snRNAs was accomplished on a 19:1 acrylamide:*bis*-acrylamide gel (long exposure), in order to separate U1 snRNA from 5.8S RNA. In agreement, with Fig 6D, each SR protein brings down trace amounts of U1 snRNA; in contrast, both CB7 (a monoclonal against U1-70K) and U1-70K-GFP bring down U1 snRNA at high levels, comparable to Y12 (anti-Sm), which IPs U1 robustly.

Table S1. Comparison of co- and post-transcriptional RNP associations of four SR proteins with different target RNAs. Shown are (Co) co-transcriptional associations based on ChIP experiments, and (N) nuclear and (C) cytoplasmic associations based RNA immunoprecipitations followed by conventional RT-PCR from uncrosslinked extracts.

Target RNA	SRp55			SC35			SRp20			9G8		
	Co	N	C	Co	N	C	Co	N	C	Co	N	C
PGK1	-	-	-	+	+	-	+	+	+	+	+	+
LDHA	-	-	-	+	+	-	-	+	+	+	+	+
HIST1	-	-	-	+	+	-	-	+	+	-	+	+
FN1	+	-	-	+	+	-	+	+	+	-	+	+
SFRS3	+	+	-	+	+	-	+	+	+	-	+	+
PTB	+	+	-	+	nd	nd	-	+	+	-	+	+
SmB	nd	+	-	nd	nd	nd	nd	+	-	nd	+	-
hnRNPA1	nd	+	-	nd	nd	nd	nd	+	+	nd	+	+